



Simulations of Indirectly Driven Gas-Filled Capsules at the National Ignition Facility

S. V. Weber, D. T. Casey, D. C. Eder, J. D. Kilkenny, J. E. Pino, V. A. Smalyuk, G. P. Grim, B. A. Remington, D. P. Rowley, C. B. Yeaman, R. E. Tipton, M. Barrios, R. Benedetti, L. B. Hopkins, D. L. Bleuel, D. K. Bradley, J. A. Caggiano, D. Callahan, C. J. Cerjan, D. S. Clark, L. Divol, D. H. Edgell, M. J. Edwards, M. J. Eckart, D. Fittinghoff, J. A. Frenje, M. Gatu-Johnson, V. Y. Glebov, S. Glenn, N. Guler, S. W. Haan, A. Hamza, R. Hatarik, H. Herrmann, D. Hoover, W. W. Hsing, N. Izumi, O. S. Jones, M. Kervin, S. Khan, J. Kline, J. Knauer, A. Kritcher, G. Kyrala, O. L. Landen, S. Le Pape, T. Ma, A. J. Mackinnon, A. G. MacPhee, M. M. Marinak, J. M. Mcnaney, N. B. Meezan, F. E. Merrill, M. Mintz, A. Moore, D. H. Munro, A. Nikroo, A. Pak, T. Parham, et al.

October 20, 2014

Physics of Plasmas

Disclaimer

This document was prepared as an account of work sponsored by an agency of the United States government. Neither the United States government nor Lawrence Livermore National Security, LLC, nor any of their employees makes any warranty, expressed or implied, or assumes any legal liability or responsibility for the accuracy, completeness, or usefulness of any information, apparatus, product, or process disclosed, or represents that its use would not infringe privately owned rights. Reference herein to any specific commercial product, process, or service by trade name, trademark, manufacturer, or otherwise does not necessarily constitute or imply its endorsement, recommendation, or favoring by the United States government or Lawrence Livermore National Security, LLC. The views and opinions of authors expressed herein do not necessarily state or reflect those of the United States government or Lawrence Livermore National Security, LLC, and shall not be used for advertising or product endorsement purposes.

Simulations of indirectly driven gas-filled capsules at the National Ignition Facility

S. V. Weber,¹ D. T. Casey,¹ D. C. Eder,¹ J. D. Kilkenny,⁵ J. E. Pino,¹ V. A. Smalyuk,¹ G. P. Grim,² B. A. Remington,¹ D. P. Rowley,¹ C. B. Yeaman,¹ R. E. Tipton,¹ M. Barrios,¹ R. Benedetti,¹ L. Berzak Hopkins,¹ D. L. Bleuel,¹ E. J. Bond,¹ D. K. Bradley,¹ J. A. Caggiano,¹ D. A. Callahan,¹ C. J. Cerjan,¹ D. S. Clark,¹ L. Divol,¹ D. H. Edgell,³ M. J. Edwards,¹ M. J. Eckart,¹ D. Fittinghoff,¹ J. A. Frenje,⁴ M. Gatu-Johnson,⁴ V. Y. Glebov,³ S. Glenn,¹ N. Guler,² S. W. Haan,¹ A. Hamza,¹ R. Hatarik,¹ H. Herrmann,² D. Hoover,⁵ W. W. Hsing,¹ N. Izumi,¹ O. S. Jones,¹ M. Kervin,¹ S. Khan,¹ J. Kline,² J. Knauer,³ A. Kritcher,¹ G. Kyrala,² O. L. Landen,¹ S. Le Pape,¹ T. Ma,¹ A. J. Mackinnon,¹ A. G. MacPhee,¹ M. M. Marinak,¹ J. M. Mcnaney,¹ N. B. Meezan,¹ F. E. Merrill,² M. Mintz,¹ A. Moore,⁶ D. H. Munro,¹ A. Nikroo,⁵ A. Pak,¹ T. Parham,¹ R. Petrasso,⁴ H. G. Rinderknecht,⁴ D. B. Sayre,¹ S. M. Sepke,¹ B. K. Spears,¹ W. Stoeffl,¹ R. Tommasini,¹ R. P. Town,¹ P. Volegov,² K. Widmann,¹ D. C. Wilson,² and A. B. Zylstra⁴

1) Lawrence Livermore National Laboratory, Livermore, CA 94550

2) Los Alamos National Laboratory, Los Alamos, NM 87545

3) Laboratory for Laser Energetics, University of Rochester, Rochester, NY 14623

4) Massachusetts Institute of Technology, Cambridge, MA 02139

5) General Atomics, San Diego, CA 92121

6) AWE Aldermaston, Reading, Berkshire, RG7 4PR, United Kingdom.

ABSTRACT

Gas-filled capsules imploded with indirect drive on the National Ignition Facility have been employed as symmetry surrogates for cryogenic-layered ignition capsules and to explore interfacial mix. Plastic capsules containing deuterated layers and filled with tritium gas provide a direct measure of mix of ablator into the gas fuel. Other plastic capsules have employed DT or D^3He gas fill. We present the results of two-dimensional simulations of gas-filled capsule implosions with known degradation sources represented as in modeling of inertial confinement fusion ignition designs; these are time-dependent drive asymmetry, the capsule support tent, roughness at material interfaces, and prescribed gas-ablator interface mix. Unlike the case of cryogenic-layered implosions, many observables of gas-filled implosions are in reasonable agreement with predictions of these simulations. Yields of TT and DT neutrons as well as other x-ray and nuclear diagnostics are matched for CD-layered implosions. Yields of DT-filled capsules are over-predicted by factors of 1.4-2, while D^3He capsule yields are matched, as well as other metrics for both capsule types.

I. INTRODUCTION

The goal of inertial confinement fusion (ICF)^{1,2} is to implode a capsule containing DT fuel so that the hot spot achieves sufficient temperature and density to ignite thermonuclear reactions and propagate into colder, denser fuel to achieve high gain. The current indirect-drive ignition design at the National Ignition Facility³⁻⁵ employs a polystyrene (CH) ablator over a layer of DT ice surrounding gas in vapor pressure equilibrium. Implosions of capsules based upon the circa-2012 ignition design gave

yields well below expectations^{6,7}, even from simulations including known sources of degradation^{8-9,11}. Layered implosions begun in 2013, using a different “high foot” laser pulse, which results in a higher adiabat¹², performed nearer to simulations. We will not discuss experiments with the high foot pulse in this report.

Capsules filled with DT gas but without a condensed DT layer provide a simpler platform to test implosion performance than cryo-layered capsules. Gas-filled capsules are known as “SymCaps” from one of their applications, as symmetry surrogates for ignition capsules. They have lower convergence, typically 15-20 as opposed to 30-40 for ignition capsules. They lack the added complexity of the frozen DT layer, which requires exquisite pulse-shaping to remain on a low adiabat, resulting in the layer becoming the pusher for stagnation. SymCaps are much less sensitive to pulse-shaping precision since the ablator is ~four times denser than DT ice to begin with. We shall see that SymCaps perform nearer to expectations than has been the case so far for cryo-layered capsules.

SymCap ablators are thickened to compensate for the mass of the missing DT ice layer. NIF They were most often filled with 30% D, 70% ³He so as to still provide nuclear diagnostic information, through the D-³He mirror reaction of DT fusion, and to increase x-ray emission compared to hydrogen fuel. Several have been fielded with DT fuel in varying isotopic proportion, allowing for wider range nuclear observables while still allowing for substantial x-ray diagnostic signal¹⁴. Recently, plastic capsules with CD layers and tritium gas fuel have been used to measure atomic mix between ablator and fuel¹⁵⁻²².

NIF SymCaps have most often been driven with the same multi-step laser pulses designed for cryo-layered ignition capsules so as to replicate the hohlraum dynamics and

consequent time-dependent symmetry of the x-ray drive. The steps are tuned so that several shocks merge just below the inner surface of the ice layer²⁴. When a gas-filled capsule is driven with the same pulse, the shocks transit the mass-equivalent CH layer in less time than the four times thicker DT ice layer and the inner surface releases before the next shock arrives, giving less than optimal compression of the ablator.

The experimental series employing CD layers and tritium gas fill is described in more detail elsewhere^{21,22}. Variations of this technique were used previously on NOVA and OMEGA¹⁵⁻²⁰. Atomic mix between the ablator and gas is needed to give DT reactions, which are diagnosed by the 14 MeV neutrons. A 4 μm thick CD layer was placed either adjacent to the gas or recessed by 1, 2, 4, or 8 μm . Earlier publications compare experimental results with the K-L dynamic mix²⁵ model in the code ARES²⁶.

In this study, we apply to SymCaps the simulation methods used to design ignition ICF capsules at LLNL³. This process is to incorporate in two-dimensional simulations using the HYDRA code the known sources of degradation: time-dependent radiation drive asymmetry, a mock-up of the effect of the capsule support tent, and resolved roughness of all interfaces. This methodology does not create atomic mix; it gives degradation by creating fingers of one material extending into another. Fingers of ablator penetrating into the capsule hot spot can cool it and degrade yield. However, fingers of CD ablator into T₂ fuel do not give DT neutrons so long as the species remain separated. Adding a mix model to the methodology is one way to rectify this deficiency.

HYDRA does not provide a dynamic mix model, i.e. one which evolves fields describing mix conditions, such as K and L, by means of differential equations. It does allow the user to specify a mix extent around interfaces, within which material species

are moved by fiat. We normalized the mix extent prescription by matching data from the CD mix experiment by varying a single scaling parameter. We were able to match data from that experiment about as well as the Ares KL model. Then we apply this model to DT and D³He-filled SymCaps. The model predicts yields larger-than-measured by about 2-3 times, but matches many other performance metrics. It is possible to match the yield if the surface roughness or growth factor is several times larger than measured, or if there is some other seed for ablation front growth which is larger in effect than surface roughness. We shall present application of our model to CD layer capsules in Section II. Extension to DT and D³He-filled gas capsules is found in Section III. Section IV gives conclusions.

II. SIMULATIONS OF IMPLOSIONS WITH CD LAYERS

The CD layer implosion series used CH capsules with a nominal diameter of 2280 μm and 209- μm thickness. Si-doped layers were used to mitigate the effect of Au M-band preheat. A CD layer of 4 μm thickness was placed next to the gas or offset by 1.2, 2.3, 3.9, or 8.0 μm . The shells were filled with tritium gas of density 11.05 mg/cm^3 with a small contamination of deuterium of about 0.1% by atom fraction. The DT yield from D contamination is a background to the signal from mix, and was measured in two shots without CD layers. Another control experiment used D_{0.75}T_{0.25} gas fill at density 8.29 mg/cm^3 . All implosions employed nominally the same laser pulse, a 4-step pulse with 1.5 MJ, peak power 435 TW, which also had been used in a number of cryo-layered DT implosions.

The performance of the implosions was measured with a multitude of nuclear and x-ray diagnostics²⁸. Hohlraum drive as measured by the Dante diagnostic²⁹ was very

repeatable, $T_r = 294 \pm 4$ eV. Capsule x-ray bang times^{30,31} were $\sim 22.55 \pm 0.10$ ns, all within 100 ps. We will focus upon capsule performance metrics of DT, DD, TT neutron yield³²⁻³⁴, neutron time-of-flight measurements³⁵ of ion temperature³⁶ and down-scatter ratio (DSR), temporal burn width from x-rays³⁷ or DT gammas^{38,39}, and x-ray⁴⁰ and neutron image size and shape⁴¹. DSR is the ratio of neutrons in the 10-12 MeV energy range to those in the 13-15 MeV range, and is diagnostic of fuel column density⁴².

Simulations with the HYDRA code were two-dimensional with axial symmetry, of the capsule only, and were driven with frequency-dependent sources linked from post-shot integrated simulations⁹. The sources included time-dependent drive asymmetry in Legendre modes up to 8 based upon capsule ablation pressure taken from the integrated simulations. The integrated simulations used measured beam quad powers for each shot. Measured backscatter was removed from the incident laser power. Cross-beam energy transfer⁴⁴ is a process where light scatters from one beam angle to another off of a plasma beat wave between the two light waves. This process is calculated with an off-line script and the incident beam powers are modified to the predicted post-transfer values. The resulting drive is still too high in comparison to match shock velocities and timing from VISAR⁴³ and capsule limb position measurements from backlit image. Those implosion energetics measurements (for shots with equivalent dimensions and pulse shapes) are matched⁹ by adjusting ad hoc time-dependent multipliers to the incident power. The effect of the 110 nm-thick capsule support web was mocked up by imposing grooves on the outside of the ablator of cosine shape, 350 μm wavelength, and 0.2 μm depth at the 45° latitude where the tent separates from the capsule. These parameters were tuned to match the appearance of the groove feature in backlit shell images at ~ 250 μm shell

radius¹⁰. Roughness at the NIF revision 5 specification³ was included on all ablator interfaces, including interfaces between dopant levels. Roughness seeded at the ablator outer surface dominated over perturbations seeded at other interfaces⁴⁵. Nuclear burn is modeled with in-line particle Monte-Carlo. Escaping particles are tallied to construct simulated neutron images and neutron spectral metrics such as down-scatter fraction and ion temperatures from DT and DD neutrons.

Because HYDRA reconstructs material interfaces, none of these perturbations would create any atomic mix between the ablator and fill gas without the addition of an interface mix model. Mix around the ablator-gas interface was imposed out to specified fractions of the separation of the “fall-line” from the interface. The fall line is the trajectory of a freely-falling particle released from the interface at the time of peak velocity, $r_{\text{fall-line}}(t) = r(t_{\text{peak}}) + v_{\text{peak}}t$, which is where the interface would have without deceleration been as a function of time. This scaling is motivated by the Rayleigh-Taylor (RT) result of Read⁴⁶ and Youngs^{47,48}

$$h_b = \alpha A g t^2$$

where h_b is the bubble height, A the Atwood number, g acceleration, t time, and α is a constant. From this it follows that the mix penetration on the bubble side is a fraction $f_b = 2\alpha A$ of the fall line separation, which is $1/2gt^2$. The ratio of penetration on the gas or “spike” side of the interface to that on the ablator or “bubble” side was specified⁴⁹ as $f_s/f_b = 1+A = 1.3$, using 0.3 as the Atwood number.

The fuel-ablator interface is subjected to series of shocks and intervals of variable acceleration of both signs so the classical RT result is not directly applicable; the fall line fraction mix prescription was employed as a convenient and physically-motivated

parameterization. Haan⁴⁹ showed that such scaling was observed for his multi-wavelength saturation model as applied to some specific cases.

The isotope fractions were constructed to be linear across the specified mix region limits. For this option, HYDRA tracks internally the material interface along each radial mesh line and automatically mixes materials in the radial mesh coordinate direction over the limits resulting from the fall line prescription. In order to couple the interface mix model with the effect of resolved perturbations, the mix boundaries were smoothed over the transverse direction with a low pass filter with a cut-off mode number of ~ 20 .

There are strengths and weaknesses of this approach as compared to the Ares KL model of references 21,22. Dynamic turbulence models which evolve two turbulent fields (K and L, for the ARES model; there are a number of such models in the literature [see discussion in 25]) are most applicable for problems in which the flow in the vicinity of an interface quickly develops into self-similar turbulence. Energy cascades down to diffusive scales. The presence of atomic mix in the CD mix experiment suggests that turbulence may be present at least in the vicinity of the ablator-gas interface.

In indirect drive ICF, growth of modulations at the ablation front is important. There, short wavelengths are stabilized by ablation and by the density gradient scale length^{50,51}, so the ablation front does not become turbulent. Weakly nonlinear modulation can feed through to the inside of the ablator where it grows further during deceleration. Cryo-layered ignition designs also have ablative stabilization between the hot-spot and main fuel, while for SymCaps the ablator-fuel boundary is a sharp material interface, so turbulence is more likely to occur. The KL model and its kin do not incorporate the physics to describe these processes with quantitative accuracy. One ignition capsule

design modeling approach^{3,8} is to address these processes by resolving the relevant scales. Computational power at this time is inadequate to resolve a turbulent cascade down to dissipative scales. Our HYDRA simulations attempt to capture the large scales, and are cut off by grid resolution for scales much shorter than the extent of the mix layer.

The KL model is intended to be predictive as long as growth is dominated by the interface acceleration history while the influence of ablation front growth is not significant. In contrast, for our fall-line based prescription, the same value of α may not apply for implosions with very different interface acceleration histories. We have chosen to normalize it to the experiment data rather than to the KL model since the two agree. We shall show later that resolved effects rather than the mix prescription are the predominant source of degradation of DT SymCaps.

Figure 1 shows material density on the right and the product of deuteron and triton number densities on the left for a typical simulation of a CD shell implosion with no offset of the CD layer. The effects of all four perturbation sources - drive asymmetry, the support tent, surface roughness, and the interface mix model – can be seen. Drive asymmetry is responsible for the prolate elongation of the shell. The structures at multiples of 45 degrees are from the tent. The smaller-scale structure in the shell was seeded by surface roughness. The interface mix model produces the thin annulus DT atomic mix of $\sim 20 \mu\text{m}$ thickness in the left half of the figure, which follows the distortion of the fuel region resulting from the other three seeds.

Figure 2(a,b) show the TT and DT yields as functions of the CD layer offset for different values of f_b . The TT yield comes from the entire gas volume and does not depend upon the location of the CD layer. The DT yield comes only from the region of

gas-ablator mix, and drops with increasing layer recession until at 8 μm recession it approaches the background due to deuterium contamination in the T_2 gas. A fall-line fraction of $f_b = 0.04$ gives a fair fit to both TT and DT experimental yields. For $A=0.3$, this corresponds to Read and Youngs $\alpha = 0.06$. Figure 2c shows the ion temperature inferred from DT neutrons. It is not possible to infer a temperature from TT neutrons because of the broad 3-body spectrum. The background experiment gave a temperature of ~ 3 keV which is a burn-weighted temperature for the entire gas volume. The DT burn temperature with the CD layer probes the mix region, which was cooler, ~ 2 keV. As the layer offset is increased, the ion temperature rises back to that of the background shots suggesting that DT yield is increasingly dominated by the contamination contribution. It cannot be inferred that mix lowered the temperature of the same mass element of gas as the DT yield came from the outer edge of the gas for the CD layer experiments compared to the entire volume for the control shots. X-ray metrics for these shots were similar to those of the corresponding DT shot N120923, which is discussed below.

The ARES model parameter fit for these shots^{21,22} used an enhanced surface roughness of three times nominal to match the experimental TT yield. Fig. 3 shows the fall-off of simulated yield for our model as the surface roughness is increased. We judge nominal roughness to be a satisfactory fit. However, the threefold nominal result matches the DT measurement better than nominal does but agrees more poorly with the TT measurement, so the overall agreement is similar to nominal roughness.

The previous analyses adjusted the roughness multiplier to fit the TT yield and the initial scale length to fit the DT yield. We adjusted the α parameter to fit both. Part of the reason that we do not need enhanced roughness results from our inclusion of the effect of

the tent and of time-dependent asymmetry, which give additional degradation besides surface roughness. Recognition of the importance of the tent effect has come from experiments performed since the preparation of the earlier reports. It is not practical to compare the KL model with the fall line prescription directly. The KL model is dynamic and gives a mix extent which grows throughout the implosion, driven by the complex acceleration history and densities on both sides of the fuel-ablator interface. The fall-line based prescription gives mix only after peak velocity and only dependent on the separation of the interface and the fall line. The two models have been normalized to give the same amount of mix at burn time to the extent that the codes agree on the clean hydrodynamics.

III. EXTENSION TO DT- AND D³HE-FILLED CAPSULES

The same simulation model was applied to four DT gas-filled implosions employing the fall line mix fraction as fit to the CD layer experiments. One, NIF shot N120923, had 75% D and 25% T but was otherwise equivalent to the CD layer shots, including its laser pulse shape. Shot N130505 used the same 439 TW peak power but with the pulse shortened to lower the energy to 1.3 MJ. Shot N130507 used lower peak power of 360 TW, but a longer pulse to give the same 1.3 MJ energy as N130505. Also, it employed a hohlraum which was 700 μm longer than those of the other shots discussed here. Shot N130503²³ used a single-shock pulse of 918 kJ in 4.3 ns with 16 torr He near-vacuum hohlraum gas fill. This implosion had lower convergence, CR \sim 6 and was nearly an exploding pusher.

Table 1 shows simulated and measured values of thirteen nuclear and x-ray diagnostic metrics for these four shots. This model reproduces the DT and DD neutron

yields, ion temperatures, gamma and x-ray burn widths, gamma and x-ray image sizes, and image elongation $P2/P0$. The simulated yields are 1.4-2 times larger than the measured values for the ablatively-driven capsules. In some cases we do not match the image shape especially well, especially N120923 where our implosion is prolate while the observed neutron image is oblate, and the x-ray image nearly round. The exploding pusher N130503 is very round both in simulation and data, while N130505 is prolate and N130507 oblate in both. Only differences exceeding about 0.1 in $P2/P0$ are likely to be meaningful. Shape tests the integrated hohlraum simulations providing the drive asymmetry rather than the capsule implosion which is the subject of this work. Our intent was to employ the best, albeit imperfect, predictive shape model available to us in order to obtain the effect of shape upon capsule performance metrics.

Ion temperatures, burn widths, down-scatter ratios, and image sizes generally agree with data nearly as well as the data is reproduced between equivalent shots. The down-scatter ratio for the exploding pusher is small and has large uncertainty. Generally, our x-ray image sizes are a little larger than measured although our neutron image sizes match measurements better. Figure 4 compares simulated and measured x-ray and neutron images for shot N120923. The simulation gets the x-ray size and elongation approximately correctly but does not predict the internal structure. Time-dependent imaging shows bright spots moving from the edge to the center, which are believed to be 3-D jets, which these simulations cannot reproduce. The simulated structure is more nearly correct for the neutron image. The 17% contour for the simulated image follows extensions toward top and bottom while similar extensions in the experimental neutron image have lower intensity and are not picked up by the 17% contour.

Figure 5 shows the progressive effect of the four degradation seeds for shot N130507. The 1-D clean yield is about 2.5 times that of the full 2-D model. Surface roughness is the largest single degradation, reducing the yield by nearly 40%. Drive asymmetry is only about a 3% effect for this case. The tent causes a 23% yield reduction in this model. Especially note that fall line mix model with $f_b=0.04$ by itself reduces the simulated yield by only 13%, a small fraction of the total degradation. Most of the yield reduction is caused by resolved structure. A different drive model from Clark⁸, which was adjusted to match inflight shell measurements, gives a yield 11% lower than the drive taken directly from integrated hohlraum simulations. The measured DT yield for this shot was 54% of the yield of the nominal 2-D model, or 61% of the yield with the Clark drive.

Figure 6 shows how the simulated DT yield of shot N130507 drops as the surface roughness is increased. The measured yield is matched at a roughness multiplier of about 5. The DD yield and ion temperature are also matched for the same multiplier. Other performance metrics listed in Table I are about the same as for nominal roughness.

Most often NIF SymCaps were fielded with D³He fill, usually in 30:70 proportion, to avoid tritium handling. There were five shots with equivalent capsules and pulses as the CD mix series. Three of these (N120906, N120909, N120910) gave DD yields of 6.06-6.99 x 10¹¹, while two had lower yields, N111120 -5.1 x 10¹¹, N120729 – 3.5 x 10¹¹. The laser pulses of all five shots agreed to within 5% in the foot, 2% in the peak. Capsule dimensions were well matched, within 14 μm in inner radius 1.5 μm in thickness. Capsule surface finishes ranged from 0.8 – 1.4 times the NIF specifications for Legendre modal bands spanning 2-25, and 0.5-0.6 times the specification for the modal

band 26-150. We were unable to identify any feature of the lower-performing shots which set them apart. It is possible that the similar yields of the three shots taken within a week were fortuitous and that NIF SymCap yields are reproducible only to within a factor 2, between extremes, for identical shots.

The shots are sufficiently similar that a single simulation applies to all five. The simulated yield of 5.5×10^{11} falls in the middle of the measured values, within 15% of three of the shots and within 40% of all. Table II compares performance metrics of shot N120909 with the model. Performance metrics besides DD yield are similar for the other four shots. Agreement of the model with performance metrics for the D³He SymCaps is quite good.

Figure 7 shows simulated and measured x-ray images for D³He fill shot N120909. The simulation captures the more centrally peaked emission for D³He fill as compared with hydrogen, as well as approximating the size and elongation of the 17% contour.

IV. CONCLUSIONS

A two-dimensional simulation model including expected degradation sources of interface roughness, time-dependent radiation drive asymmetry, a mock up of the support tent, and an interface mix prescription is able to match the performance of tritium-filled capsules with a CD layer recessed different distances from the interface with the fill gas. The same model matches the performance of capsules filled with D³He gas. The model also matches many performance metrics of capsules with DT gas fill. However, the model over-predicts the DT yield of those capsules by up to a factor of two.

The yields of the ablatively-driven DT capsules can be matched by increasing the surface roughness in the models by a factor of about 5. This factor does not seem to be

necessary for TT or D³He-filled capsules. This could be evidence of isotope separation⁵², or perhaps these three specific shots performed more poorly, like the D³He shot N120729. Clark et al.⁸ found that a factor of 5 enhancement in roughness matched the yield of a specific DT-layered capsule, which was more than a factor of 10 below the prediction for nominal roughness. Layered capsules are much more sensitive to degradation sources, likely because of higher convergence and otherwise differing dynamics from gas-filled implosions.

The capsules employed for these shots could not have been this rough, but the growth factors of perturbations could be higher than simulated or there could be additional growth seeds not represented in the model. The calculated growth factor of ablation front perturbations to the time of peak velocity is ~1000 for these SymCaps⁵³, so an additional factor of 5 is only 20% more e-foldings of growth. Spike penetration in 3-D is expected to be larger than 2-D only by perhaps 50% in the nonlinear regime⁵⁴, not enough to account for the discrepancy.

One might ask whether the mix prescription employed in this study would affect simulated performance of layered implosions. Unfortunately, the interface mix prescription used here for gas-filled capsules has little effect upon the yield of layered implosions which do not ignite, such as all those to date for NIF. The hot spot in layered implosions is separated from the ablator by cold DT, so mix of modest extent about the inner surface of the ablator does not penetrate into the hot spot. The yield of an igniting capsule would be degraded by pollution of the cold fuel. There is no material interface between the cold DT and the hot spot about which an analogous mix prescription could be used, and ablative stabilization acts against the development of turbulence.

Ongoing experiments are measuring growth of applied surface perturbations to test the growth predicted by simulations⁵⁵. Efforts to improve drive symmetry and reduce the effect of the tent are also under way. However, a pronounced improvement in yield may not be apparent in gas-filled capsules because their performance may not be sufficiently sensitive. Only cryo-layered implosions may confirm definitively the improvement in implosion uniformity.

ACKNOWLEDGMENTS

This work would not be possible without the efforts of a very large team of NIF diagnostic scientists, operations staff, target fabricators, and program management.

This work was performed under the auspices of the U.S. Department of Energy by Lawrence Livermore National Laboratory under Contract DE-AC52-07NA27344.

REFERENCES

¹S. Atzeni and J. Meyer-ter-Vehn, *The Physics of Inertial Fusion: Beam Plasma Interaction, Hydrodynamics, Hot Dense Matter*, International Series of Monographs on Physics (Clarendon Press, Oxford, 2004).

²J. D. Lindl, *Inertial Confinement Fusion: The Quest for Ignition and Energy Gain Using Indirect Drive* (Springer-Verlag, New York, 1998).

³S. W. Haan, J. D. Lindl, D. A. Callahan, D. S. Clark, J. D. Salmonson, B. A. Hammel, L. J. Atherton, R. C. Cook, M. J. Edwards, S. Glenzer, A. V. Hamza, S. P. Hatchett, M. C. Herrmann, D. E. Hinkel, D. D. Ho, H. Huang, O. S. Jones, J. Kline, G. Kyrala, O. L. Landen, B. J. MacGowan, M. M. Marinak, D. D. Meyerhofer, J. L. Milovich, K. A. Moreno, E. I. Moses, D. H. Munro, A. Nikroo, R. E. Olson, K. Peterson, S. M. Pollaine, J. E. Ralph, H. F. Robey, B. K. Spears, P. T. Springer, L. J. Suter, C. A. Thomas, R. P.

Town, R. Vesey, S. V. Weber, H. L. Wilkens, and D. C. Wilson *Phys. Plasmas* **18**, 051001 (2011).

⁴E. I. Moses, R. N. Boyd, B. A. Remington, C. J. Keane, and R. Al-Ayat, *Phys. Plasmas* **16**, 041006 (2009);

⁵G. H. Miller, E. I. Moses and C. R. Wuest, *Opt. Eng.* **443**, 2841 (2004).

⁶S. P. Regan, R. Epstein, B. A. Hammel, L. J. Suter, J. Ralph, H. Scott, M. A. Barrios, D. K. Bradley, D. A. Callahan, C. Cerjan, G. W. Collins, S. N. Dixit, T. Doeppner, M. J. Edwards, D. R. Farley, S. Glenn, S. H. Glenzer, I. E. Golovkin, S. W. Haan, A. Hamza, D. G. Hicks, N. Izumi, J. D. Kilkenny, J. L. Kline, G. A. Kyrala, O. L. Landen, T. Ma, J. J. MacFarlane, R. C. Mancini, R. L. McCrory, N. B. Meezan, D. D. Meyerhofer, A. Nikroo, K. J. Peterson, T. C. Sangster, P. Springer and R. P. J. Town, *Phys. Plasmas* **19**, 056307 (2012).

⁷T. Ma, P.K. Patel, N. Izumi, P.T. Springer, M.H. Key, L.J. Atherton, L.R. Benedetti, D.K. Bradley, D.A. Callahan, P.M. Celliers, C.J. Cerjan, D.S. Clark, E.L. Dewald, S.N. Dixit, T. Doppner, D.H. Edgell, R. Epstein, S. Glenn, G. Grim, S.W. Haan, B.A. Hammel, D. Hicks, W.W. Hsing, O.S. Jones, S.F. Khan, J.D. Kilkenny, J.L. Kline, G.A. Kyrala, O.L. Landen, S. Le Pape, B.J. MacGowan, A.J. Mackinnon, A.G. MacPhee, N.B. Meezan, J.D. Moody, A. Pak, T. Parham, H.-S. Park, J.E. Ralph, S.P. Regan, B.A. Remington, H.F. Robey, J.S. Ross, B.K. Spears, V. Smalyuk, L.J. Suter, R. Tommasini, R.P. Town, S.V. Weber, J.D. Lindl, M.J. Edwards, S.H. Glenzer, and E.I. Moses, *Phys. Rev. Lett.* **111**, 085004 (2013).

⁸D. S. Clark, D. E. Hinkel, D. C. Eder, O. S. Jones, S. W. Haan, B. A. Hammel, M. M. Marinak, J. L. Milovich, H. F. Robey, L. J. Suter and R. P. J. Town, *Phys. Plasmas* **20**, 056318 (2013).

⁹O. S. Jones, C. J. Cerjan, M. M. Marinak, J. L. Milovich, H. F. Robey, P. T. Springer, L. R. Benedetti, D. L. Bleuel, E. J. Bond, D. K. Bradley, D. A. Callahan, J. A. Caggiano, P. M. Celliers, D. S. Clark, S. M. Dixit, T. Doppner, R. J. Dylla-Spears, E. G. Dzentitis, D. R. Farley, S. M. Glenn, S. H. Glenzer, S. W. Haan, B. J. Haid, C. A. Haynam, D. G. Hicks, B. J. Koziolowski, K. N. LaFortune, O. L. Landen, E. R. Mapoles, A. J. MacKinnon, J. M. McNaney, N. B. Meezan, P. A. Michel, J. D. Moody, M. J. Moran, D. H. Munro, M. V. Patel, T. G. Parham, J. D. Sater, S. M. Sepke, B. K. Spears, R. P. J. Town, S. V. Weber, K. Widmann, C. C. Widmayer, E. A. Williams, L. J. Atherton, M. J. Edwards, J. D. Lindl, B. J. MacGowan, L. J. Suter, R. E. Olson, H. W. Herrmann, J. L. Kline, G. A. Kyrala, D. C. Wilson, J. Frenje, T. R. Boehly, V. Glebov, J. P. Knauer, A. Nikroo, H. Wilkens and J. D. Kilkenny, *Phys. Plasmas* **19**, 056315 (2012).

¹⁰S. W. Haan, L. Berzak Hopkins, D. S. Clark, D. Eder, B. A. Hammel, A. Hamza, D. Ho, O. S. Jones, A. Kritcher, K. LaFortune, B. J. MacGowan, N. B. Meezan, J. Milovich, J. L. Peterson, H. F. Robey, J. D. Salmonson, B. K. Spears, R. P. Town, J. L. Kline, D. C. Wilson, A. N. Simakov, S. A. Yi, A. Nikroo, H. Huang and H. Hoover, *Bull. Am. Phys. Soc.* **58**, 155 (2013).

¹¹B. K. Spears, S. Glenzer, M. J. Edwards, S. Brandon, D. Clark, R. Town, C. Cerjan, R. Dylla-Spears, E. Mapoles, D. Munro, J. Salmonson, S. Sepke, S. Weber, S. Hatchett, S. Haan, P. Springer, E. Moses, J. Kline, G. Kyrala and D. Wilson, *Phys. Plasmas* **19**, 056316 (2012).

¹²O. A. Hurricane, D. A. Callahan, D. T. Casey, P. M. Celliers, C. Cerjan, E. L. Dewald, T. R. Dittrich, T. Döppner, D. E. Hinkel, L. F. Berzak Hopkins, J. L. Kline, S. Le Pape, T. Ma, A. G. MacPhee, J. L. Milovich, A. Pak, H.-S. Park, P. K. Patel, B. A. Remington, J. D. Salmonson, P. T. Springer and R. Tommasini, *Nature* 13008 (2014).

¹³G. A. Kyrala, J. L. Kline, S. Dixit, S. Glenzer, D. Kalantar, D. Bradley, N. Izumi, N. Meezan, O. Landen, D. Callahan, S. V. Weber, J. P. Holder, S. Glenn, M. J. Edwards, J. Koch, L. J. Suter, S. W. Haan, R. P. J. Town, P. Michel, O. Jones, S. Langer, J. D. Moody, E. L. Dewald, T. Ma, J. Ralph, A. Hamza, E. Dzenitis, and J. Kilkenny, *Phys. Plasmas* **18**, 056307 (2011).

¹⁴J. D. Kilkenny, J. A. Caggiano, R. Hatarik, J. P. Knauer, D. B. Sayre, B. K. Spears, S. V. Weber, C. B. Yeamans, C. J. Cerjan, L. Divol, M. J. Eckart, V. Yu. Glebov, H. W. Herrmann, S. Le Pape, D. H. Munro, G. P. Grim, O. S. Jones, L. Berzak-Hopkins, M. Gatu-Johnson, A. J. Mackinnon, N. B. Meezan, D. T. Casey, J. A. Frenje, J. M. McNaney, R. Petrasso, H. Rinderknecht, W. Stoeffl and A. B. Zylstra, “Understanding the stagnation and burn of implosions on NIF”, 2013 IFSA proceedings, in press (2014).

¹⁵D. C. Wilson, P. S. Ebey, T. C. Sangster, W. T. Shmayda, V. Yu. Glebov and R. A. Lerche, *Phys. Plasmas* **18**, 112707 (2011).

¹⁶D. D. Meyerhofer, J. A. Delettrez, R. Epstein, V. Yu. Glebov, V. N. Goncharov, R. L. Keck, R. L. McCrory, P. W. McKenty, F. J. Marshall, P. B. Radha, S. P. Regan, S. Roberts, W. Seka, S. Skupsky, V. A. Smalyuk, C. Sorce, C. Stoeckl, J. M. Soures, R. P. J. Town, B. Yaakobi, J. D. Zuegel, J. Frenje, C. K. Li, R. D. Petrasso, F. H. Séguin, K. Fletcher, S. Padalino, C. Freeman, N. Izumi, R. Lerche, T. W. Phillips and T. C. Sangster, *Phys. Plasmas* **8**, 2251 (2001).

¹⁷P. B. Radha, J. Delettrez, R. Epstein, V. Yu Glebov, R. Keck, R. L. McCrory, P. McKenty, D. D. Meyerhofer, F. Marshall, S. P. Regan, S. Roberts, T. C. Sangster, W. Seka, S. Skupsky, V. Smalyuk, C. Sorce, C. Stoeckl, J. Soures, R. P. J. Town, B. Yaakobi, J. Frenje, C. K. Li, R. Petrasso, F. Seguin, K. Fletcher, S. Padalino, C. Freeman, N. Izumi, R. Lerche and T. W. Phillips, *Phys. Plasmas* **9**, 2208 (2002).

¹⁸C. K. Li, F. H. Séguin, J. A. Frenje, S. Kurebayashi, R. D. Petrasso, D. D. Meyerhofer†, J. M. Soures, J. A. Delettrez, V. Yu. Glebov, P. B. Radha, S. P. Regan, S. Roberts, T. C. Sangster, and C. Stoeckl, *Phys. Rev. Lett.* **89**, 165002 (2002).

¹⁹J. R. Rygg, J. A. Frenje, C. K. Li, F. H. Séguin, R. D. Petrasso, V. Yu. Glebov, D. D. Meyerhofer†, T. C. Sangster, and C. Stoeckl, *Phys. Rev. Lett.* **98**, 215002 (2007).

²⁰R. E. Chrien, N. M. Hoffman, J. D. Colvin, C. J. Keane, O. L. Landen and B. A. Hammel, *Phys. Plasmas* **5**, 768 (1998).

²¹V. A. Smalyuk, R. E. Tipton, J. E. Pino, D. T. Casey, G. P. Grim, B. A. Remington, D. P. Rowley, S. V. Weber, M. Barrios, R. Benedetti, D. L. Bleuel, D. K. Bradley, J. A. Caggiano, D. A. Callahan, C. J. Cerjan, D. S. Clark, D. H. Edgell, M. J. Edwards, J. A. Frenje, M. Gatu-Johnson, V. Y. Glebov, S. Glenn, S. W. Haan, A. Hamza, R. Hatarik, W. W. Hsing, N. Izumi, S. Khan, J. D. Kilkenny, J. Kline, J. Knauer, O. L. Landen, T. Ma, J. M. McNaney, M. Mintz, A. Moore, A. Nikroo, A. Pak, T. Parham, R. Petrasso, D. B. Sayre, M. B. Schneider, R. Tommasini, R. P. Town, K. Widmann, D. C. Wilson, and C. B. Yeamans *Phys. Rev. Lett.* **112**, 025002 (2014).

²²D. T. Casey, V. A. Smalyuk, R. E. Tipton, J. E. Pino, G. P. Grim, B. A. Remington, D. P. Rowley, S. V. Weber, M. Barrios, R. Benedetti, D. L. Bleuel, E. J. Bond, D. K. Bradley, J. A. Caggiano, D. A. Callahan, C. J. Cerjan, D. H. Edgell, M. J. Edwards, D.

Fittinghoff, J. A. Frenje, M. Gatu-Johnson, V. Y. Glebov, S. Glenn, N. Guler, S. W. Haan, A. Hamza, R. Hatarik, H. Herrmann, D. Hoover, W. W. Hsing, N. Izumi, P. Kervin, S. Khan, J. D. Kilkenny, J. Kline, J. Knauer, G. Kyrala, O. L. Landen, T. Ma, J. M. McNaney, M. Mintz, A. Moore, A. Nikroo, A. Pak, T. Parham, R. Petrasso, H. G. Rinderknecht, D. B. Sayre, M. Schneider, R. Tommasini, R. P. Town, K. Widmann, D. C. Wilson, and C. B. Yeamans, *Phys. Plasmas* **21**, 092705 (2014).

²³S. Le Pape, L. Divol, L. Berzak Hopkins, A. Mackinnon, N. B. Meezan, D. Casey, J. Frenje, H. Herrmann, J. McNaney, T. Ma, K. Widmann, A. Pak, G. Grimm, J. Knauer, R. Petrasso, A. Zylstra, H. Rinderknecht, M. Rosenberg, M. Gatu-Johnson, and J. D. Kilkenny. *Phys. Rev. Lett.* **112**, 225002 (2014).

²⁴D. H. Munro, P. M. Celliers, G. W. Collins, D. M. Gold, L. B. Da Silva, S. W. Haan, R. C. Cauble, B. A. Hammel, and W. W. Hsing, *Phys. Plasmas* **8**, 2245 (2001).

²⁵G. Dimonte and R. Tipton, *Phys. Fluids* **18**, 085101 (2006).

²⁶R. M. Darlington, T. L. McAbee, and G. Rodrigue, *Comput. Phys. Commun.* **135**, 58 (2001).

²⁷M. M. Marinak, R. E. Tipton, O. L. Landen, T. J. Murphy, P. Amendt, S. W. Haan, S. P. Hatchett, C. J. Keane, R. McEachern, and R. Wallace, *Phys. Plasmas* **3**, 2070 (1996).

²⁸M. G. Johnson, J. A. Frenje, D. T. Casey, C. K. Li, F. H. Séguin, R. Petrasso, R. Ashabranner, R. M. Bionta, D. L. Bleuel, E. J. Bond, J. A. Caggiano, A. Carpenter, C. J. Cerjan, T. J. Clancy, T. Doeppner, M. J. Eckart, M. J. Edwards, S. Friedrich, S. H. Glenzer, S. W. Haan, E. P. Hartouni, R. Hatarik, S. P. Hatchett, O. S. Jones, G. Kyrala, S. Le Pape, R. A. Lerche, O. L. Landen, T. Ma, A. J. MacKinnon, M. A. McKernan, M. J. Moran, E. Moses, D. H. Munro, J. McNaney, H. S. Park, J. Ralph, B. Remington, J. R.

Rygg, S. M. Sepke, V. Smalyuk, B. Spears, P. T. Springer, C. B. Yeamans, M. Farrell, D. Jasion, J. D. Kilkenny, A. Nikroo, R. Paguio, J. P. Knauer, V. Yu Glebov, T. C. Sangster, R. Betti, C. Stoeckl, J. Magoon, M. J. Shoup III, G. P. Grim, J. Kline, G. L. Morgan, T. J. Murphy, R. J. Leeper, C. L. Ruiz, G. W. Cooper and A. J. Nelson, *Rev. Sci. Instrum.* **83**, 10D308 (2012).

²⁹ E.L. Dewald, K.M. Campbell, R.E. Turner, J.P. Holder, O.L. Landen, S.H. Glenzer, R.L. Kauffman, L.J. Suter, M. Landon, M. Rhodes, D. Lee, “Dante soft x-ray power diagnostic for National Ignition Facility“, *Rev. Sci. Instrum.*, **75**, 3759, (2004).

³⁰ A G MacPhee, D H Edgell, E J Bond, D K Bradley, C G Brown, S R Burns, J R Celeste, C J Cerjan, M J Eckart, V Y Glebov, S H Glenzer, D S Hey, O S Jones, J D Kilkenny, J R Kimbrough, O L Landen, A J Mackinnon, N B Meezan, J M Parker and R M Sweeney, *J. Instrum.* **6**, P02009 (2011).

³¹ M. A. Barrios, A. MacPhee, S. P. Regan, J. Kimbrough, S. R. Nagel, L. R. Benedetti, S. F. Khan, D. Bradley, P. Bell, D. Edgell and G. W. Collins, *Rev. Sci. Instrum.* **83**, 10E105 (2012)

³² D. L. Bleuel, C. B. Yeamans, L. A. Bernstein, R. M. Bionta, J. A. Caggiano, D. T. Casey, G. W. Cooper, O. B. Drury, J. A. Frenje, C. A. Hagmann, R. Hatarik, J. P. Knauer, M. Gatu Johnson, K. M. Knittel, R. J. Leeper, J. M. McNaney, M. Moran, C. L. Ruiz and D. H. G. Schneider, *Rev. Sci. Instrum.* **83**, 10D313 (2012).

³³ C. B. Yeamans, D. L. Bleuel and L. A. Bernstein, *Rev. Sci. Instrum.* **83**, 10D315 (2012).

³⁴ D. T. Casey, J. A. Frenje, M. Gatu Johnson, F. H. Séguin, C. K. Li, R. D. Petrasso, V. Yu. Glebov, J. Katz, J. P. Knauer, D. D. Meyerhofer, T. C. Sangster, R. M. Bionta, D. L. Bleuel, T. Döppner, S. Glenzer, E. Hartouni, S. P. Hatchett, S. Le Pape, T. Ma, A.

MacKinnon, M. A. Mckernan, M. Moran, E. Moses, H.-S. Park, J. Ralph, B. A. Remington, V. Smalyuk, C. B. Yeaman, J. Kline, G. Kyrala, G. A. Chandler, R. J. Leeper, C. L. Ruiz, G. W. Cooper, A. J. Nelson, K. Fletcher, J. Kilkenny, M. Farrell, D. Jasion and R. Paguio, *Rev. Sci. Instrum.* **83**, 10D912 (2012).

³⁵R. Hatarik, J. A. Caggiano, V. Glebov, J. McNaney, C. Stoeckl and D. H. G. Schneider, *Plas. Fus. Res.: Regular Articles* **9**, 0001000 (2014).

³⁶H. Brysk, *Plasma Phys.* **15**, 611 (1973).

³⁷S. F. Khan; P. M. Bell; D. K. Bradley; S. R. Burns; J. R. Celeste; L. S. Dauffy; M. J. Eckart; M. A. Gerhard; C. Hagmann; D. I. Headley; J. P. Holder; N. Izumi; M. C. Jones; J. W. Kellogg; H. Y. Khater; J. R. Kimbrough; A. G. Macphee; Y. P. Opachich; N. E. Palmer; R. B. Petre; J. L. Porter; R. T. Shelton; T. L. Thomas; J. B. Worden, in *Target Diagnostics Physics and Engineering for Inertial Confinement Fusion*, eds. P. Bell and G. P. Grim, *Proc. SPIE* **8505**, 850505 (2012).

³⁸D. B. Sayre, L. A. Bernstein, J. A. Church, H. W. Herrmann and W. Stoeffl, *Rev. Sci. Instrum.* **83**, 10D905 (2012).

³⁹R. M. Malone, H. W. Herrmann, W. Stoeffl, J. M. Mack and C. S. Young, *Rev. Sci. Instrum.* **79**, 10E532 (2008).

⁴⁰S. M. Glenn, L. R. Benedetti, D. K. Bradley, B. A. Hammel, N. Izumi, S. F. Khan, G. A. Kyrala, T. Ma, J. L. Milovich, A. E. Pak, V. A. Smalyuk, R. Tommasini and R. P. Town, *Rev. Sci. Instrum.* **83**, 10E519 (2012).

⁴¹F. E. Merrill, D. Bower, R. Buckles, D. D. Clark, C. R. Danly, O. B. Drury, J. M. Dzenitis, V. E. Fatherley, D. N. Fittinghoff, R. Gallegos, G. P. Grim, N. Guler, E. N. Loomis, S. Lutz, R. M. Malone, D. D. Martinson, D. Mares, D. J. Morley, G. L. Morgan,

J. A. Oertel, I. L. Tregillis, P. L. Volegov, P. B. Weiss, C. H. Wilde and D. C. Wilson, *Rev. Sci. Instrum.* **83**, 10D317 (2012).

⁴²D.C. Wilson, W.C. Mead, L. Disdier, M. Houry, J.-L. Bourgade, T.J. Murphy, *Nucl. Instr. Meth. Phys. Res. Sec. A*, **488**, 400 (2002).

⁴³P. M. Celliers, D. K. Bradley, G. W. Collins, D. G. Hicks, T. R. Boehly, and W. J. Armstrong, *Rev. Sci. Instrum.* **75**, 4916 (2004); R. M. Malone, J. R. Bower, G. A. Capelle, J. R. Celeste, P. M. Celliers, B. C. Frogget, R. L. Guyton, M. I. Kaufman, G. A. Lare, T. L. Lee, B. J. MacGowan, S. Montelongo, E. W. Ng, T. L. Thomas, Jr., T. W. Tunnell, and P. W. Watts, *Proc. SPIE* **5523**, 148 (2004).

⁴⁴P. Michel, L. Divol, E. A. Williams, S. Weber, C. A. Thomas, D. A. Callahan, S. W. Haan, J. D. Salmonson, S. Dixit, D. E. Hinkel, M. J. Edwards, B. J. MacGowan, J. D. Lindl, S. H. Glenzer, and L. J. Suter, *Phys. Rev. Lett.* **102**, 025044-1-4 (2009).

⁴⁵D. S. Clark, S. W. Haan, A. W. Cook, M. J. Edwards, B. A. Hammel, J. M. Koning and M. M. Marinak, *Phys. Plasmas* **18**, 082701 (2011).

⁴⁶K. I. Read, *Physica* **D12**, 45 (1984).

⁴⁷D. L. Youngs *Physica* **D12**, 32 (1984).

⁴⁸D. L. Youngs, *Physica* **D37**, 270 (1989).

⁴⁹S. W. Haan, *Phys. Rev. A* **39**, 5812 (1989).

⁵⁰H. Takabe, K. Mima, L. Montierth, and R. L. Morse, *Phys. Fluids* **28**, 3676 (1985).

⁵¹R. Betti, V. N. Goncharov, R. L. McCrory, P. Sorokin and C. P. Verdon, *Phys. Plasmas* **3**, 2122 (1996).

⁵²C. Bellei, P. A. Amendt, S. C. Wilks, M. G. Haines, D. T. Casey, C. K. Li, R. Petrasso and D. R. Welch *Phys. Plasmas* **20**, 012701 (2013)

⁵³B. A. Hammel, H. A. Scott, S. P. Regan, C. Cerjan, D. S. Clark, M. J. Edwards, R. Epstein, S. H. Glenzer, S. W. Haan, N. Izumi, J. A. Koch, G. A. Kyrala, O. L. Landen, S. H. Langer, K. Peterson, V. A. Smalyuk, L. J. Suter, and D. C. Wilson, *Phys. Plasmas* **18**, 056310 (2011).

⁵⁴M. M. Marinak, S. G. Glendinning, R. J. Wallace, B. A. Remington, K. S. Budil, S. W. Haan, R. E. Tipton, and J. D. Kilkenny, *Phys. Rev. Lett.* **80**, 4426 (1998).

⁵⁵V. A. Smalyuk, M. Barrios, J. A. Caggiano, D. T. Casey, C. J. Cerjan, D. S. Clark, M. J. Edwards, J. A. Frenje, M. Gatu-Johnson, V. Y. Glebov, G. Grim, S. W. Haan, B. A. Hammel, A. Hamza, D. E. Hoover, W. W. Hsing, O. Hurricane, J. D. Kilkenny, J. L. Kline, J. P. Knauer, J. Kroll, O. L. Landen, J. D. Lindl, T. Ma, J. M. McNaney, M. Mintz, A. Moore, A. Nikroo, T. Parham, J. L. Peterson, R. Petrasso, L. Pickworth, J. E. Pino, K. Raman, S. P. Regan, B. A. Remington, H. F. Robey, D. P. Rowley, D. B. Sayre, R. E. Tipton, S. V. Weber, K. Widmann, D. C. Wilson and C. B. Yeamans, *Phys. Plasmas* **21**, 056301 (2014).

Table I. DT capsule performance

metric	N120923	N120923 simulation	N130503	N130503 simulation	N130505	N130505 simulations	N130507	N130507 simulation
DT Y	6.7e14	1.08e15	5.1e14	5.48e14	8.0e14	1.12e15	7.3e14	1.45e15
DT Ti (keV)	3.3	3.06	4.62	4.83	2.72	2.99	2.81	3.14
DD Y	7.53e12	1.28e13	1.54e12	1.84e12	3e12	4.54e12	2.82e12	5.45e12
DD Ti (keV)	3.12	2.87	4.19	4.34	2.45	2.81	2.36	2.94
dsr (%)	1.1	1.0	0.25	0.10	1.16	1.00	1.06	1.11
γ BT (ns)	22.42	22.51	4.64	4.77	22.68	22.77	23.37	23.37
x-ray BT (ns)	22.47	22.52	4.90	4.88	22.83	22.79	23.46	23.39
γ BW (ps)	245	219	340	365	269	243	295	219
x-ray BW (ps)	243	243	373	208	380	302	313	239
x-ray P0 (μ m)	44.3	51.3	181	182		57.4	40.1	50.5
x-ray P2/P0 (%)	-0.4	27	-2	1.1		53	-27.9	-14.7
n image P0 (μ m)	46	48.2	100	106	50.3	51.3	39	46.3
n image P2/P0 (%)	-19	20	2		27	37	-28	-7.4

DT yield – yield of escaping neutrons in 13-15 MeV energy range, DT Ti – ion temperature inferred from width of 14 MeV neutron peak, DD Y – yield of escaping neutrons in 2.2-2.7 MeV energy range, DD Ti – ion temperature inferred from width of DD peak, dsr – down-scatter ratio, 10-12 MeV / 13-15 MeV neutrons; BT – bang time; BW – burn full width at half maximum; P0,P2 – Legendre modes of image contour at 17% of peak; neutron image metrics are for primary 14 MeV neutron image. Not all data exists for some shots.

Table II. D³He capsule performance

metric	N120909	simulation
DD Y	6.06e11	5.45e11
DD Ti (keV)	2.45	2.39
x-ray BT (ns)	22.59	22.48
x-ray BW (ps)	266	267
x-ray P0 (μm)	51.0	47.2
x-ray P2/P0 (%)	4.8	-5.3

Items as in Table I.

FIGURE CAPTIONS

FIG. 1. Right-simulated density at bang time for nominal drive for the CD SymCap shot series, coordinates in cm, ordinate is symmetry axis (vertical on NIF), color scale (g/cm^2) as shown; left-normalized product of deuterium and tritium number densities at bang time for an ablator with a zero offset CD layer, color scale going from zero to one.

FIG. 2. (a) Simulated DT neutron yield vs. recess of the CD layer with (i) $f_b=0$, (ii) $f_b=0.04$, (iii) $f_b=0.08$, (iv) $f_b=0.16$. Shot data points are solid circles; two overlapping background shots with no CD layer plotted on left, simulation using $f_b=0.04$ as the open circle. In most cases, error bars are smaller than the symbols; (b) TT neutron yield vs. recess of the CD layer, symbols as in (a); (c) Ion temperature from 14 MeV DT peak vs recess of the CD layer, symbols as in (a).

FIG. 3. Simulated DT and TT neutron yields vs. multiplier applied to nominal surface roughness for CD SymCap with zero layer offset, using best fit $f_b=0.04$. The dashed and dotted lines are the measure DT and TT yields, respectively.

FIG. 4. (a) Simulated primary neutron image of shot N120923; red line is 17% isocontour, scale is in μm . (b) Simulated x-ray image of shot N120923 at peak brightness through 2.5 mm kapton filter. (c) Experimental primary neutron image of N130923. (d) Experimental x-ray image of N120923 at peak brightness through 2.5 mm kapton filter.

FIG. 5. Simulated DT yield for shot N130507 as degradations are added progressively from 1-D clean, 2-d with surface roughness only, adding drive asymmetry, adding the tent mock-up, adding the mix model with $f_b=0.04$, and 2-d with all seeds and a different drive model developed by Dan Clark⁸. At the bottom is the measured DT yield.

FIG. 6. Simulated DT yield for shot N130507 vs. multiplier applied to nominal surface roughness. These results use a slightly different drive model than Fig. 5 and Table I. The observed yield is indicated with the dashed line.

FIG. 7. (a) Simulated x-ray image of D³He-filled SymCap, shot N120909, at peak x-ray emission, filtered with 2.5 mm kapton, scale is in μm ; (b) experimental x-ray image of N120909 at peak x-ray brightness. Contour levels are 17% of peak.

Figure 1

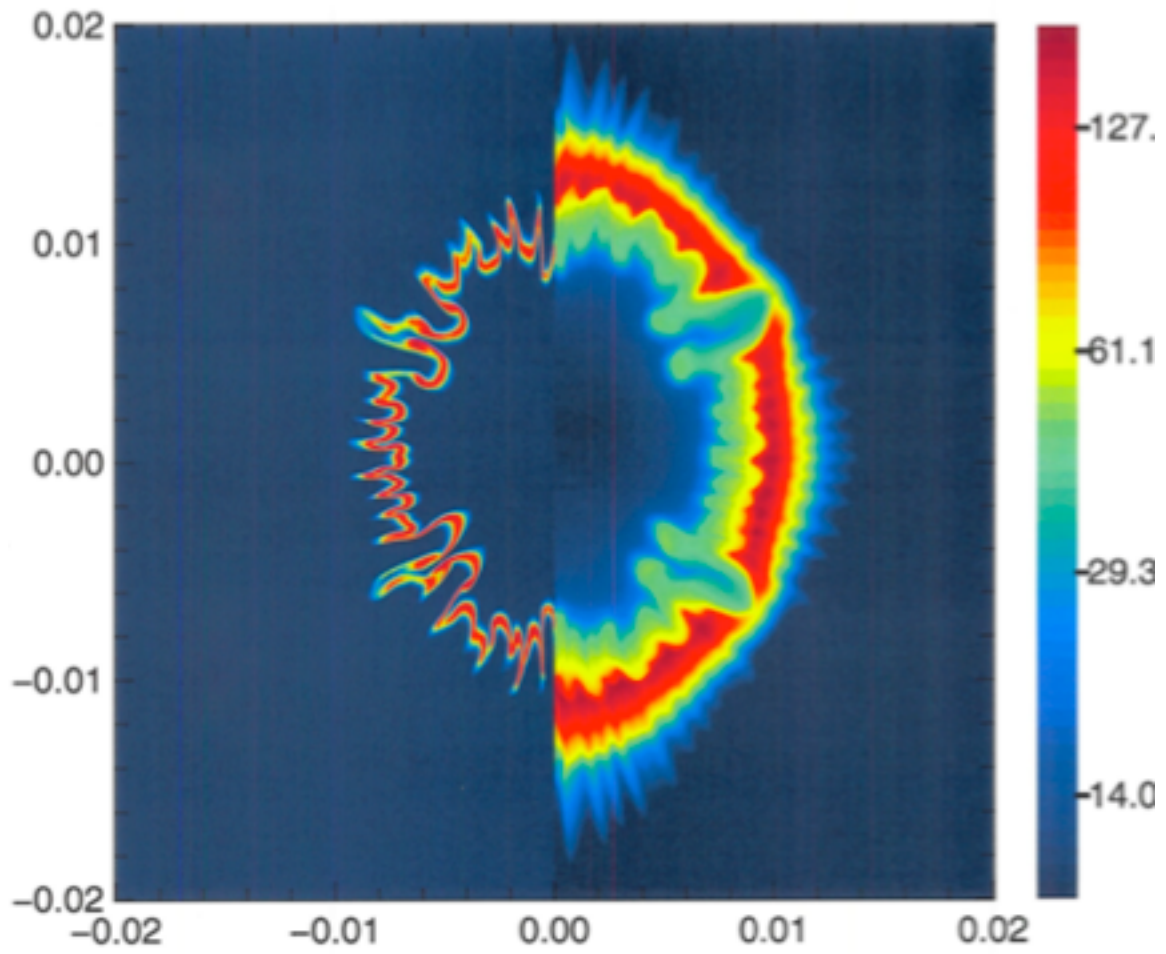
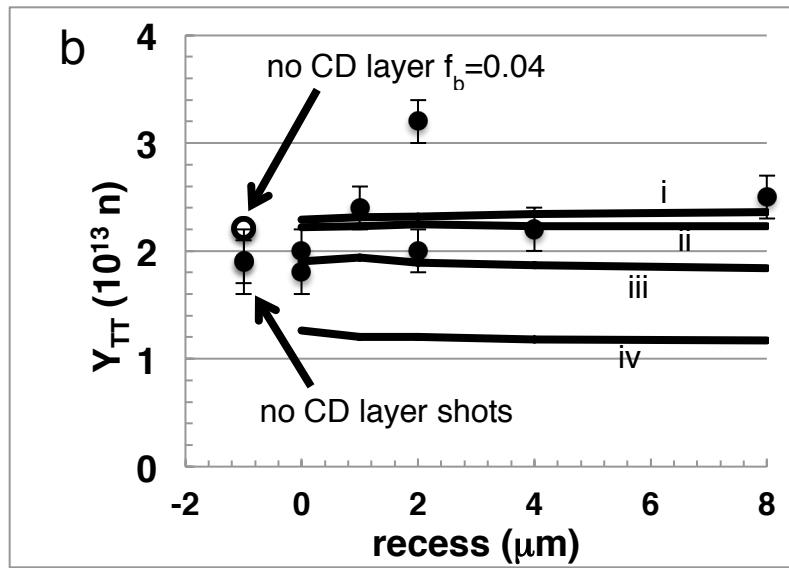
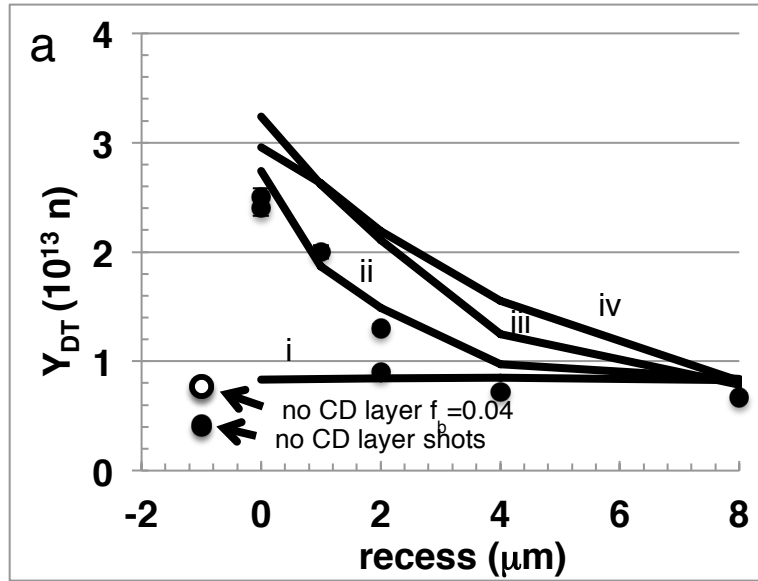


Figure 2



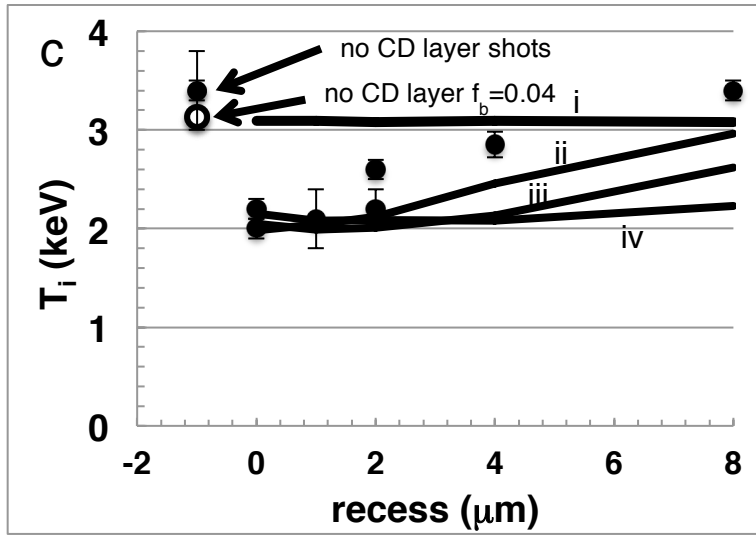


Figure 3

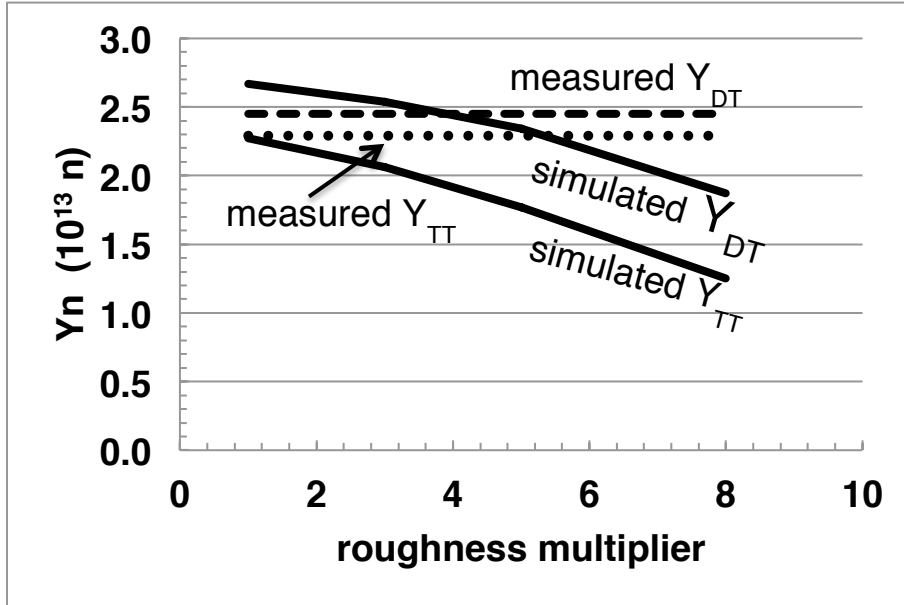


Figure 4

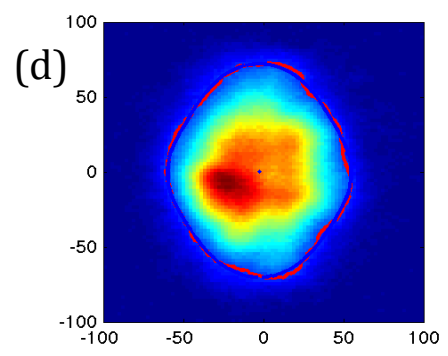
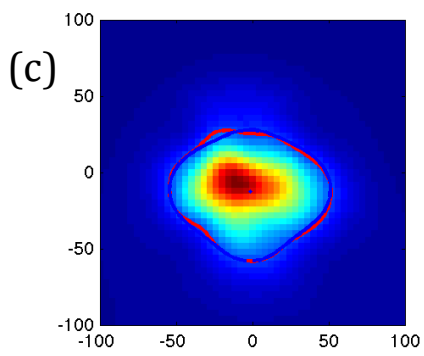
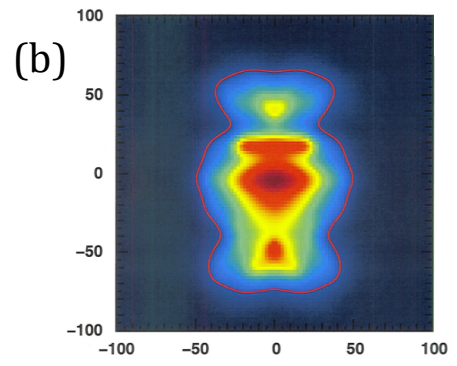
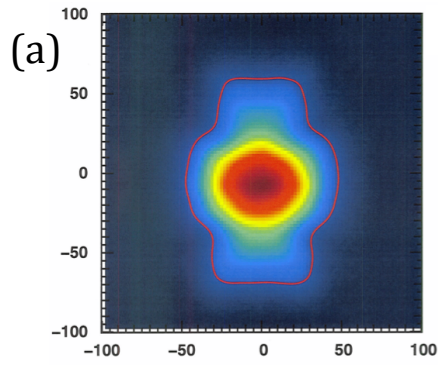


Figure 5

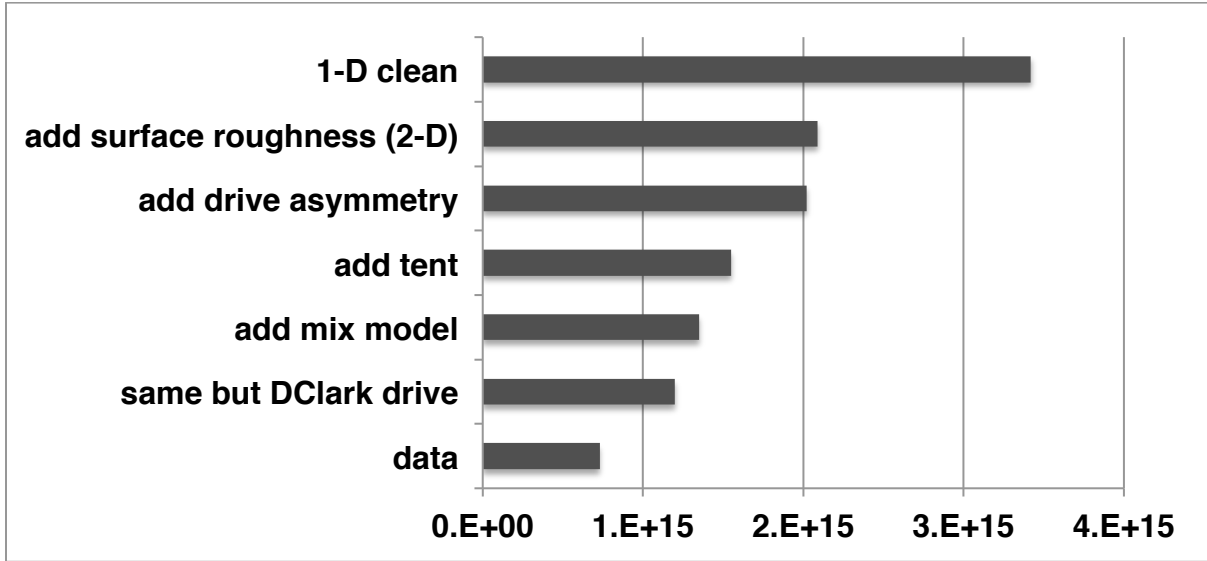


Figure 6

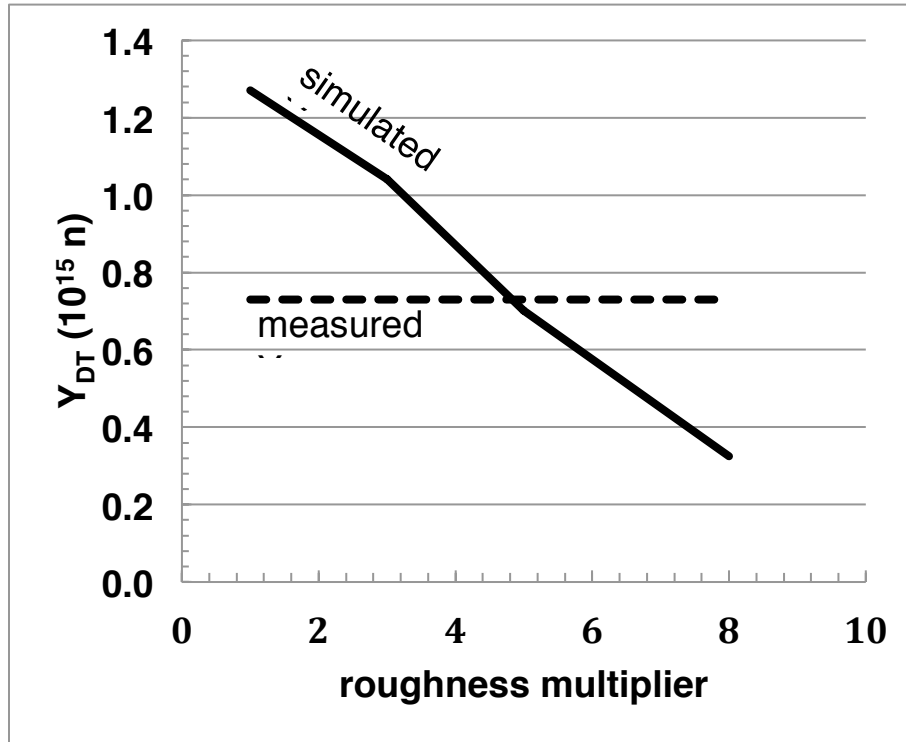


Figure 7

